Available online at www.sciencedirect.com

ScienceDirect

journal homepage: www.elsevier.com/locate/he

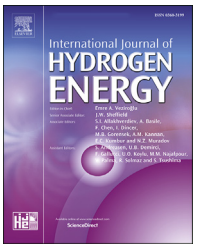

Thermodynamic analysis of a tri-generation system using SOFC and HDH desalination unit

Hamid Reza Abbasi [b], *Hossein Pourrahmani* [a,*], *Nazanin Chitgar* [b], *Jan Van herle* [a]

[a] *Group of Energy Materials (GEM), École Polytechnique Fédérale de Lausanne, Sion 1951, Switzerland*
[b] *School of Mechanical Engineering, Iran University of Science and Technology, Tehran, Iran*

HIGHLIGHTS

- Suggesting a novel system to produce freshwater, electricity, and cooling.
- Thermodynamic analysis of the proposed novel tri-generation system.
- Having energy and exergy efficiencies of 60% and 55%, respectively.
- Parametric study considering the changes in the SOFC's current density.

ARTICLE INFO

Article history:
Received 21 February 2021
Received in revised form
19 April 2021
Accepted 25 April 2021
Available online xxx

Keywords:
Thermodynamic analysis
Solid oxide fuel cell (SOFC)
Kalina cycle
Liquefied natural gas (LNG)
Humidification-dehumidification (HDH)
Reverse osmosis (RO)

ABSTRACT

The lack of freshwater in many countries pushes authorities to utilize desalination units. Solid Oxide Fuel Cells (SOFC) have shown promising results to provide the power to establish a multi-generation system using hydrogen as a renewable source. In this article, to better improve the efficiency of the suggested integrated system, the waste heat of the SOFC is recovered through the application of a Kalina power cycle and Humidification-dehumidification (HDH) desalination unit. Liquefied Natural Gas (LNG) cold stream also utilizes the waste heat of the Kalina cycle (KC) to provide cooling and power simultaneously. As all the considered cycles of Kalina, LNG cold stream, and SOFC can produce power and as this amount of electricity would be higher than the grid's demand, a further Reverse Osmosis (RO) desalination unit is utilized to increase the output amount of freshwater in the proposed system. The main focus of this study is to perform the thermodynamic analysis of this tri-generation system, which can generate power, cooling, and freshwater. Results indicate that the exergy and energy efficiencies of the current suggested system when the current density of the SOFC is 550 (A/m^2), is around 55% and 60%, respectively.

Introduction

Nowadays, the growing demand of industries and people for energy with current fossil fuel resources being limited is one of the major challenges. These types of fuels suffer from high output emissions and may not be the best economic option, which is pushing towards environmentally friendly fuel alternatives [1–5]. Hybrid systems using renewable energies

* *Corresponding author.*
E-mail address: hossein.pourrahmani@epfl.ch (H. Pourrahmani).

https://doi.org/10.1016/j.ijhydene.2021.04.152

have proved to be efficient compared to conventional fossil fuel integrated systems [6].

Fuel cells that use renewable fuels have shown promising results to be a suitable replacement for fossil fuel-based devices [7]. A fuel cell is capable to generate electrical power through an electrochemical reaction [8]. Due to its superior advantages including high efficiency, low emission, and flexibility in fuel consumption, this technology has become a source of competitive power generation compared to conventional and well-established prime movers such as engines and turbines [9]. Considering the operating temperature, fuel cells are in two main categories of high- and low-temperature [10–12].

Solid oxide fuel cells (SOFC) have been widely developed due to its significant potentials such as high efficiency and flexibility in using different fuels at high temperatures, which makes them suitable for multi-generation purposes [13,14]. Using a novel system, Yang et al. [15] could propose a system with a near-zero CO_2 emission. The exergy efficiency, CO_2 capture rate, and energy efficiency were 64.7%, 98.7%, and 54.4%, respectively. Comparing the operation of a single gas turbine (GT) unit with a hybrid SOFC-GT system, Haseli et al. [16] showed 26.6% and 27.8% improvement in the energy and exergy efficiencies, respectively, when a hybrid system is being used. Saebea et al. [17] analyzed different renewable fuels as the input of the SOFC and concluded that glycerol is the best option for SOFC-H^+ integrated system. Paulson et al. [18] verified the higher performance of a SOFC-GT hybrid system with a sensitivity analysis. The results of this study showed that a lower pressure ratio leads to an electrical efficiency of more than 65%. Despite the recovery of SOFC's exhaust by GT, the SOFC-GT output stream is still at a high temperature, which can be used to integrate technologies that operate with low- and medium-grade heat sources.

Among the developed technologies, the Kalina Cycle (KC) and Organic Rankine Cycle (ORC) that use a mixture of ammonia-water and organic fluid as the working fluid, respectively, are viable alternatives for converting low- and medium-temperature heat sources into electrical power. The evaporation of the water-ammonia mixture decreases the irreversibilities [19] and results in a better performance of the KC compared to an ORC [20,21]. Ma et al. [22] suggested a hybrid system that the dissipated heat of SOFC-GT is introduced to a KC to generate surplus electricity and reach a system efficiency of more than 80%. The results demonstrated that a higher fuel flow rate enhances the overall conversion efficiency, while high pressure ratio leads to improved electrical efficiency and conversion efficiency. Soltani et al. [23] evaluated different types of working fluids for different types of ORC and KC and concluded that R290 can be the best possible option as the working fluid, to enhance the waste heat recovery and to increase the production capacity by 2.47%.

Although the KC can recover waste heat sources efficiently, the waste heat from the KC by itself becomes considerable on some occasions, and devising an approach to obviate this problem is valuable. Integration of this cycle with cooling cycles such as an absorption refrigeration cycle [24,25], ejector refrigeration [26], and cold sources of energy such as an LNG cold stream [27,28] has been successful to increase the efficiency of a multi-generation system. In this regard, a cooling capacity would be produced, which can be used for domestic usage [29], and the generated electricity by the LNG turbine can be utilized to run a RO unit.

Reverse osmosis (RO) desalination units [30] have been commercialized due to their industrial capabilities (low capital investment cost and energy use). These units, which consume electricity, have been vastly utilized in the Middle-East to meet water demands. Chitgar et al. [31] investigated the possibility of integrating SOFC, GT, and KC-TEG into a combined cycle using a RO desalination unit to produce freshwater. Results indicated that the exergy efficiency and the total cost rate are 54% and 36.8 $/hr, respectively, in optimal conditions. Mokhtari et al. [32] suggested a hybrid system using Multi-Effect Desalination (MED) and RO units to provide the water demand of 10304.3 $\frac{m^3}{day}$in a city close to the Persian Gulf. Sadri et al. [33] also evaluated a similar integration of MED-RO using the irreversibility concept. The developed research by Eshoul et al. [34] indicated that a higher recovery ratio of a RO unit results in lower exergy destructions, hence higher efficiencies. Altmann et al. [35] compared 48 different types of cogeneration systems to produce freshwater and electricity simultaneously and concluded that RO desalination is the most energy-efficient system. Although RO units can provide freshwater using electricity [36], finding another desalination system to recover waste heat would be needed in some applications.

Herein, the application of a RO unit together with a humidification-dehumidification (HDH) [37,38] desalination unit, which is driven by heat, can completely provide the needs of freshwater in different applications. Low maintenance cost, and simple manufacturing are the other advantages of a HDH unit [39]. The integration of this thermally based desalination unit with solar collectors [40] lead to the production of 12 m^3 considering 1.88 MWh/year solar irradiance. A more detailed analysis considering the environmental and economical aspects was developed by Deniz et al. [41] on a similar hybrid system to produce 1117.3 g/h freshwater. The integration of SOFC and HDH was previously analyzed by Ghaebi et al. [42] and concluded that the SOFC stack and the afterburner are the highest exergy destruction among the utilized components.

The focus of this study is to propose a novel multi-generation system to simultaneously produce power, freshwater, and cooling. The main purpose of integrated systems is to increase the energy and exergy efficiencies while reducing the waste heat of the whole system. The waste heat of a SOFC, used partly by the KC, still has enough energy to run an HDH desalination unit, and the waste heat would thus be minimized. Although typical desalination units use electricity to work, devising HDH unit enables the direct recovery of heat to freshwater. In parallel working of HDH and RO units, facilitates the freshwater production using both heat and electricity as inputs. Furthermore, Kalina cycle can increase the output generated electricity by the system while enables the usage of LNG cold stream on its condenser to provide cooling for domestic applications. The current suggested integrated system has not been proposed and evaluated so far, and analyzing this system enables the decision makers to select the right system for their application. Although other tri-generation systems have been proposed so far to

Please cite this article as: Abbasi HR et al., Thermodynamic analysis of a tri-generation system using SOFC and HDH desalination unit, International Journal of Hydrogen Energy, https://doi.org/10.1016/j.ijhydene.2021.04.152

produce freshwater, cooling, and electricity, this combination has neither been proposed nor analyzed yet. Thermodynamic analysis of this combination has been performed to better evaluate the suitability of this system. Energy and exergy analysis have been separately developed for different current densities of the SOFC in two conditions of the standalone SOFC and integrated system. The variation of freshwater production, cooling capacity, and SOFC power with the variation in current density is shown as well. Finally, the rates of exergy destruction for each component of the system have been clearly mentioned to better evaluate the efficiency of the system.

Problem description

The suggested multi-generation system, which produces power, cooling, and freshwater, encompasses five different cycles (see Fig. 1). In this system, a solid oxide fuel cell (SOFC) produces electricity using methane as fuel. Reforming occurs in the anode to produce the needed hydrogen for the electrochemical reactions. The heat of these reactions increases the temperature of the output gas from the SOFC, which can be recovered using a KC and HDH desalination unit. This output hot gas from the after-burner of a SOFC evaporates the ammonia-water mixture in a KC and heats the seawater to be sprayed in the humidifier of a HDH unit.

The working fluid of KC has a constant amount of water and ammonia, however, it's mass fraction changes in some processes of this cycle due to the existence of the separator. At first, the received heat from SOFC increases the temperature of the ammonia-water mixture in the evaporator of the KC. Then, the ammonia will be separated from the water in a separator to produce electricity in a turbine while the separated fluid gives its thermal energy to the output cold mixture of the KC's pump in a recuperator. After, these two separated fluids get mixed together again and give their remaining thermal energy to the LNG cold stream in the condenser. It should be noted that the overall amount of ammonia and water is constant in the Kalina cycle and only their mass fractions change due to the usage of separator, hence the composition does not change and the system is stable. The produced cooling capacity from this stream can be used for domestic application while the generated electricity by its turbine in addition to the output electricity of the SOFC and of the KC, provide grid power and the electricity required to run the RO desalination unit. The three existing turbines of the system provide the required pumping power for the KC, LNG stream, and RO unit. The SOFC unit is responsible to generate power for the air compressor, fuel compressor, and water pump, and excess power is directed to the grid.

Thermodynamic modeling

To analyze the energetic and exergetic performances of the current suggested integration of the system, mathematical

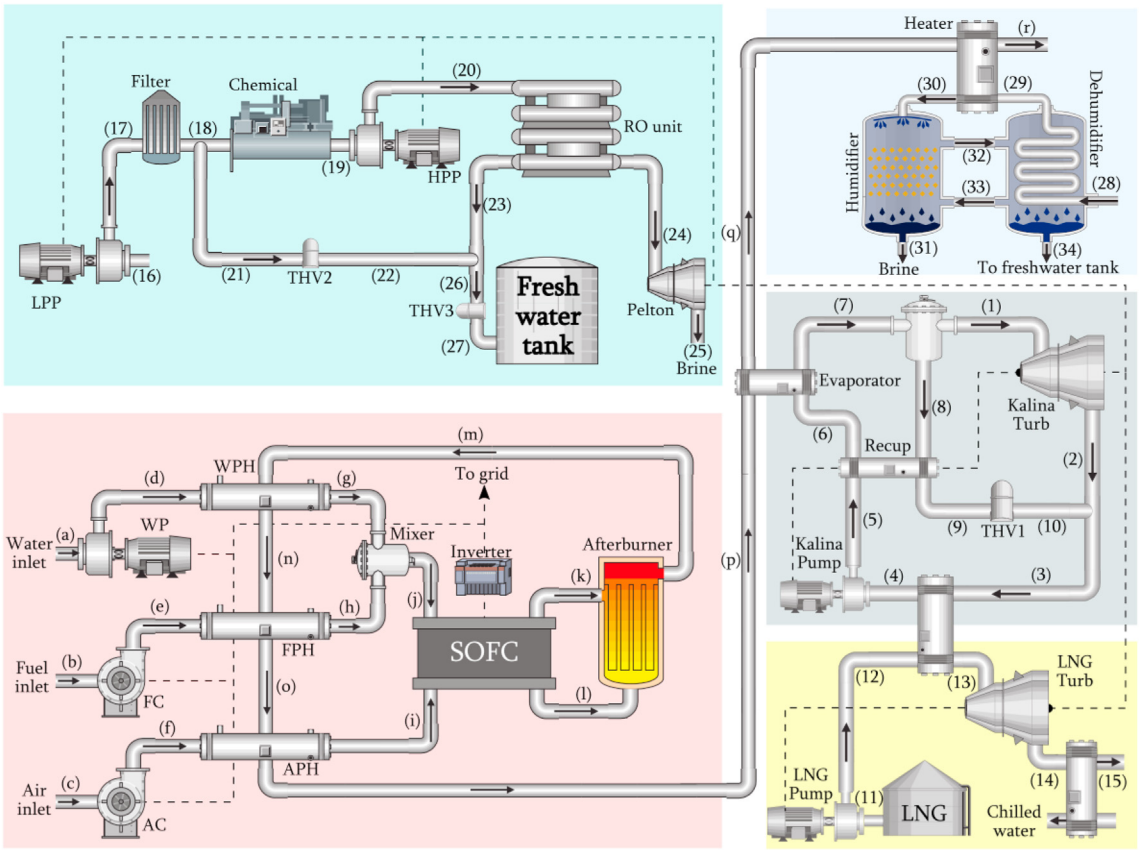

Fig. 1 – A schematic of the tri-generation thermal system.

Please cite this article as: Abbasi HR et al., Thermodynamic analysis of a tri-generation system using SOFC and HDH desalination unit, International Journal of Hydrogen Energy, https://doi.org/10.1016/j.ijhydene.2021.04.152

modeling, and thermodynamic analysis is needed. This modeling has been developed considering the steady-state condition, negligible pressure drops and losses of heat in the pipes, and inconsiderable variations of the potential and kinetic energies.

Solid oxide fuel cell (SOFC)

As the SOFC utilizes hydrogen as the fuel, methane should enter a reformer first. In this regard, the methane changes to hydrogen based on the reforming reaction, shown in Eq. (1), respectively. Then, electricity can be generated in the SOFC stack based on the overall chemical reaction (see Eq. (2)

$$CH_4 + H_2O \leftrightarrow 3H_2 + CO \tag{1}$$

$$H_2 + \frac{1}{2}O_2 \rightarrow H_2O \tag{2}$$

The output power of the SOFC stack is a parameter of the number of the cells (N_{cell}), activation area (A_{act}), and the cell's voltage (V_{cell}):

$$\dot{W}_{SOFC} = iA_{act}N_{cell}V_{cell} \tag{3}$$

where (i) is the current density and Eq. (4) presents V_{cell} using the reversible voltage (V_N) and voltage losses (V_{loss}). The detailed values of these parameters are mentioned by Chitgar et al. [31], where ζ_{ohm}, ζ_{act}, and ζ_{conc} are the ohmic, activation, and concentration overpotentials, respectively.

$$V_{cell} = V_N - V_{loss} \tag{4}$$

$$V_{loss} = \zeta_{ohm} + \zeta_{act} + \zeta_{conc} \tag{5}$$

Kalina cycle (KC)

As mentioned before, the output heat of the SOFC stack would be first recovered by the KC followed by the HDH unit. In the first step, the working fluid of KC (ammonia-water) vaporizes following relation (6):

$$\dot{m}_G(h_p - h_q) = \dot{m}_6(h_7 - h_6) \tag{6}$$

where $\dot{m}_G$ is the mass flow rate of output water from the SOFC stack. After separating the mixture in the separator (Eqs. (7) and (8)), the power can be produced in the turbine (see Eq. (9)).

$$\dot{m}_7 h_7 = \dot{m}_8 h_8 + \dot{m}_1 h_1 \tag{7}$$

$$\dot{m}_7 X_7 = \dot{m}_8 X_8 + \dot{m}_1 X_1 \tag{8}$$

$$\dot{W}_{turb} = \dot{m}_1(h_1 - h_2) \tag{9}$$

Table 1 – Input and output values of exergy for different components of the integrated system.

Component	Exergy balance equation
Fuel cell group	
SOFC stack	$\dot{E}x^{ch}_{(j)} + \dot{E}x^{ph}_{(j)} + \dot{E}x^{ch}_{(i)} + \dot{E}x^{ph}_{(i)} = \dot{E}x^{ph}_{(k)} + \dot{E}x^{ch}_{(k)} + \dot{E}x^{ph}_{(l)} + \dot{E}x^{ch}_{(l)} + \dot{E}x_{D,SOFC}$
Air compressor	$\dot{E}x_{(c)} + \dot{W}_{(AC)} = \dot{E}x_{(f)} + \dot{E}x_{D,comp}$
Fuel compressor	$\dot{E}x_{(b)} + \dot{W}_{(FC)} = \dot{E}x_{(e)} + \dot{E}x_{D,comp}$
Water pump	$\dot{E}x_{(a)} + \dot{W}_{(WP)} = \dot{E}x_{(d)} + \dot{E}x_{D,pump}$
Air preheater	$\dot{E}x_{(o)} + \dot{E}x_{(f)} = \dot{E}x_{(i)} + \dot{E}x_{(p)} + \dot{E}x_{D,APH}$
Fuel preheater	$\dot{E}x_{(n)} + \dot{E}x_{(e)} = \dot{E}x_{(h)} + \dot{E}x_{(o)} + \dot{E}x_{D,FPH}$
Water preheater	$\dot{E}x_{(m)} + \dot{E}x_{(d)} = \dot{E}x_{(g)} + \dot{E}x_{(n)} + \dot{E}x_{D,WPH}$
Mixer	$\dot{E}x_{(g)} + \dot{E}x_{(h)} = \dot{E}x_{(j)} + \dot{E}x_{D,mixer}$
Afterburner	$\dot{E}x_{(k)} + \dot{E}x_{(l)} = \dot{E}x_{(m)} + \dot{E}x_{D,afterburner}$
Kalina system	
Evaporator	$\dot{E}x_{(p)} + \dot{E}x_6 = \dot{E}x_{(q)} + \dot{E}x_7 + \dot{E}x_{D,evap}$
Separator	$\dot{E}x_7 = \dot{E}x_1 + \dot{E}x_8 + \dot{E}x_{D,sep}$
Turbine	$\dot{E}x_1 = \dot{E}x_2 + \dot{W}_{turbine} + \dot{E}x_{D,turbine}$
Recuperator	$\dot{E}x_8 + \dot{E}x_5 = \dot{E}x_9 + \dot{E}x_6 + \dot{E}x_{D,recup}$
THV1	$\dot{E}x_9 = \dot{E}x_{10} + \dot{E}x_{D,tv}$
Pump	$\dot{E}x_4 + \dot{W}_{pump} = \dot{E}x_5 + \dot{E}x_{D,pump}$
Water heater	$\dot{E}x_3 + \dot{E}x_{12} = \dot{E}x_4 + \dot{E}x_{13} + \dot{E}x_{D,con}$
LNG cooling	
Turbine	$\dot{E}x_{13} = \dot{E}x_{14} + \dot{W}_{turbine} + \dot{E}_{D,turbine}$
Cooling unit	$\dot{E}x_{13} = \dot{E}x_{14} - \dot{E}x_{Q,vap} + \dot{E}x_{D,con}$
Pump	$\dot{E}x_{11} + \dot{W}_{pump} = \dot{E}x_{12} + \dot{E}x_{D,pump}$
HDH unit	
Humidifier	$\dot{E}x_{30} + \dot{E}x_{33} = \dot{E}x_{31} + \dot{E}x_{32} + \dot{E}x_{D,humidifier}$
Dehumidifier	$\dot{E}x_{32} + \dot{E}x_{28} = \dot{E}x_{33} + \dot{E}x_{29} + \dot{E}x_{D,dehumidifier}$
RO unit	
RO module	$\dot{E}x_{20} = \dot{E}x_{23} + \dot{E}x_{24} + \dot{E}x_{D,RO}$
LP pump	$\dot{E}x_{16} + \dot{W}_{LPP} = \dot{E}x_{17} + \dot{E}x_{D,LPP}$
HP pump	$\dot{E}x_{19} + \dot{W}_{HPP} = \dot{E}x_{20} + \dot{E}x_{D,HPP}$
Pelton turbine	$\dot{E}x_{24} = \dot{E}x_{25} + \dot{W}_{Pelton} + \dot{E}x_{D,Pelton}$
THV2	$\dot{E}x_{21} = \dot{E}x_{22} + \dot{E}x_{D,tv}$
THV3	$\dot{E}x_{26} = \dot{E}x_{27} + \dot{E}x_{D,tv}$

Please cite this article as: Abbasi HR et al., Thermodynamic analysis of a tri-generation system using SOFC and HDH desalination unit, International Journal of Hydrogen Energy, https://doi.org/10.1016/j.ijhydene.2021.04.152

The separated liquid in the separator flows to the recuperator and transfers the heat to the pumped mixture from the condenser as follows:

$$\dot{m}_8(h_9 - h_8) = \dot{m}_5(h_6 - h_5) \quad (10)$$

Then, this liquid passes the THV1 (see Eq. (11)) and is mixed again with the output flow of the turbine (see Eq. (12)).

$$h_9 = h_{10} \quad (11)$$

$$\dot{m}_2 h_2 + \dot{m}_{10} h_{10} = \dot{m}_3 h_3 \quad (12)$$

The remaining heat of the fluid would be used in the LNG stream using the condenser as a low temperature heat exchanger:

$$\dot{m}_3(h_4 - h_3) = \dot{m}_{11}(h_{13} - h_{12}) \quad (13)$$

At the end the fluid would be pumped again to increase the pressure and flowing to the evaporator:

$$\dot{W}_{pump} = \dot{m}_4(h_5 - h_4) \quad (14)$$

LNG cold stream

The pressure of the stored liquid LNG in the tank increases by a pump (see Eq. (15)) to pass the condenser of the KC to change the state to a gas (see Eq. (13)).

$$\dot{W}_{LNG,pump} = \dot{m}_{11}(h_{12} - h_{11}) \quad (15)$$

Table 2 – Operating parameters of the integrated system.

Cycle	Parameter	Value
SOFC system	Inlet temperature (K)	900
	Fuel utilization factor (%)	85
	Current density (mA/cm^2)	550
	Active surface area (m^2)	0.01
	Number of cells (–)	55,000
	Number of electrons (–)	2
	Exchange current density of anode (mA/cm^2)	650
	Exchange current density of cathode (mA/cm^2)	250
	Effective gaseous diffusivity, anode (m^2/s)	0.2×10^{-4}
	Effective gaseous diffusivity, cathode (m^2/s)	0.05×10^{-4}
	Anode thickness (m)	0.05×10^{-2}
	Cathode thickness (m)	0.005×10^{-2}
	Electrolyte thickness (m)	0.105×10^{-2}
	Interconnect thickness (m)	0.3×10^{-2}
	Steam-to-carbon ratio (–)	2.5
	Efficiency of fuel compressor (%)	85
	Efficiency of air compressor (%)	85
	Fuel cell pressure drop (%)	2
	Heat exchangers pressure drop (%)	2
	Afterburner pressure drop (%)	3
LNG	Inlet temperature (K)	111.15
	Inlet pressure (kPa)	101.325
	Pump pressure ratio (–)	12
Kalina cycle	Pinch point temperature difference (PPTD) in evaporator (K)	25
	Terminal temperature difference (TTD) in evaporator (K)	25
	Basic ammonia mass fraction (–)	0.7
	Turbine inlet pressure (kPa)	3000
	Evaporation temperature (K)	$T_{(p)}$-TTD
	Condensation temperature (K)	293.15
	Turbine efficiency (%)	85
	Pump efficiency (%)	75
	PPTD in recuperator (K)	10
RO unit	High pressure pump efficiency (%)	90
	Low pressure pump efficiency (%)	87
	Pelton efficiency (%)	79
	Recovery ratio of RO unit (–)	0.55
	Membrane salt rejection ratio (–)	0.99
	Seawater temperature (K)	298.15
	Seawater salinity (ppm)	35,000
HDH unit	Relative humidity of air (%)	90
	Water-to-air mass flow ratio (–)	2.333
	Top temperature (K)	353.15
	Bottom temperature (K)	298.15
	Heater TTD (K)	5
	Hum. and Deh. effectiveness (%)	85

Please cite this article as: Abbasi HR et al., Thermodynamic analysis of a tri-generation system using SOFC and HDH desalination unit, International Journal of Hydrogen Energy, https://doi.org/10.1016/j.ijhydene.2021.04.152

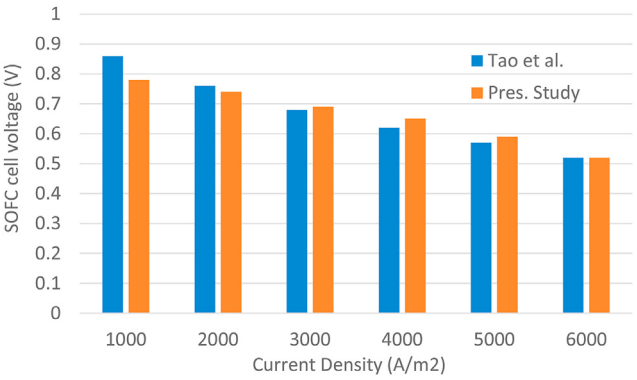

Fig. 2 – Model validation of the SOFC comparing to the experimental results of Tao et al. [43].

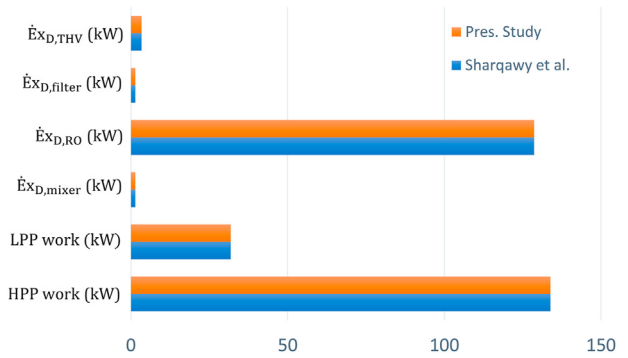

Fig. 3 – Model validation of the RO unit with the reported results by Sharqawy et al. [45].

The utilized turbine can produce further power for the RO unit as follows:

$$\dot{W}_{LNG,turb} = \dot{m}_{11}(h_{14} - h_{13}) \tag{16}$$

The output cooling amount of the LNG stream can be obtained through the cooling unit as follows:

$$\dot{Q}_{cooling} = \dot{m}_{11}(h_{15} - h_{14}) \tag{17}$$

HDH unit

The main components of the HDH unit are the heater, humidifier, and dehumidifier. The heater (see Eq. (18)) exchanges the energy of the working fluid while the mass and energy transfers happen in the humidifier (see Eq. (19)) and the dehumidifier (see Eq. (20)).

$$\dot{Q}_H = \dot{m}_{30}h_{30} - \dot{m}_{29}h_{29} \tag{18}$$

$$\dot{m}_{31}h_{31} - \dot{m}_{30}h_{30} = \dot{m}_{da}(h_{33} - h_{32}) \tag{19}$$

$$\dot{m}_{29}h_{29} - \dot{m}_{28}h_{28} + \dot{m}_{34}h_{34} = \dot{m}_{da}(h_{32} - h_{33}) \tag{20}$$

Here $\dot{m}_{da}$ indicates the mass flow rate of the dried air. Considering the output energy content to the obtained energy through heat transfer in the heater, the gained output ratio (GOR) can be calculated:

$$GOR = \frac{\dot{m}_{34}h_{fg}}{\dot{Q}_H} \tag{21}$$

here h_{fg} is the water latent heat of vaporization.

RO unit

Among the available desalination units, which work using electricity, RO units have shown promising results. Considering y_s as the mass fraction of the salt, Eqs. (22) and (23) calculate the salinity of brine and freshwater as follows:

$$(\dot{m}y_s)_{20} = (\dot{m}y_s)_{23} + (\dot{m}y_s)_{24} \tag{22}$$

$$(\dot{m}y_s)_{23} = (\dot{m}y_s)_{22} + (\dot{m}y_s)_{26} \tag{23}$$

Herein, the plant recovery ratio is considered to be the ratio of the product water to that of feed water as follows:

$$R_r = \frac{\dot{m}_{product}}{\dot{m}_{feed}} = \frac{\dot{m}_{27}}{\dot{m}_{25}} \tag{24}$$

Additionally, Eq. (25) calculates the bypass mass flow rate using the conservation principle in the mixing chamber:

$$\dot{m}_{21} = \dot{m}_{26}\left(\frac{y_{s,26} - y_{s,23}}{y_{s,21} - y_{s,23}}\right) \tag{25}$$

Exergy equations

To figure out the performance of each component in the integrated system and their ability to produce the work, exergy analysis is needed. In this regard, chemical (e_{ch}) and physical (e_{ph}) exergies should be determined, then, using the exergy balance equations (see Table 1) the exergy destructions can be calculated. For a determined substance, the exergy (ex) can be calculated as follows:

$$ex = e_{ch} + e_{ph} \tag{26}$$

Herein, physical exergy (see Eq. (27)) indicates the maximum work potential obtainable by taking the mass stream at thermal and mechanical equilibrium with the environment while the chemical exergy (see Eq. (28)) is a result of changes in the mass fraction of the working fluid.

$$e_{ph} = (h - h_0) - T_0(s - s_0) \tag{27}$$

$$e_{ch} = \left[\frac{e_{ch}^{-0}, NH_3}{M_{NH_3}}\right]y + \left[\frac{e_{ch}^{-0}, H_2O}{M_{H_2O}}\right] \tag{28}$$

Eq. (29) also presents the contribution of the k_{th} component in total exergy destruction as follows:

$$Y_k^* = \frac{\dot{E}x_{D,k}}{\dot{E}x_{D,total}} \tag{29}$$

In the end, the overall efficiencies should be determined to measure the performance of the system and compare it to the other proposed systems. Eqs. (30) and (31) present the overall energy and exergy efficiencies, respectively:

Please cite this article as: Abbasi HR et al., Thermodynamic analysis of a tri-generation system using SOFC and HDH desalination unit, International Journal of Hydrogen Energy, https://doi.org/10.1016/j.ijhydene.2021.04.152

Table 3 – Thermodynamic properties of the SOFC.

State	T (K)	P (kPa)	$\dot{n}$ (mol/s)	mole fraction percentage						
				CH4	H2O	H2	CO	CO2	O2	N2
a	298.15	101	6.41	0	100	0	0	0	0	0
b	298.15	101	2.46	100	0	0	0	0	0	0
c	298.15	121	194.83	0	0	0	0	0	21.00	79.00
d	298.15	121	6.41	0	100	0	0	0	0	0
e	314.84	121	2.46	100	0	0	0	0	0	0
f	316.02	118	194.83	0	0	0	0	0	21.00	79.00
g	900	118	6.41	0	100	0	0	0	0	0
h	900	118	2.46	100	0	0	0	0	0	0
i	900	118	194.83	0	0	0	0	0	21.00	79.00
j	900	116	8.87	27.78	72.22	0	0	0	0	0
k	946.44	116	14.13	0	71.18	10.68	1.40	16.75	0	0
l	946.44	112	190.59	0	0	0	0	0	19.24	80.76
m	1008.8	110	203.80	0	5.66	0	0	1.26	17.56	75.52
n	947.3	108	203.80	0	5.66	0	0	1.26	17.56	75.52
o	935.8	106	203.80	0	5.66	0	0	1.26	17.56	75.52
p	394.03	106	203.80	0	5.66	0	0	1.26	17.56	75.52
q	381.26	106	203.80	0	5.66	0	0	1.26	17.56	75.52

Table 4 – Thermodynamic properties of the KC-LNG-RO-HDH.

State	Composition	T (K)	P (kPa)	$\dot{E}x$ (kW)	$\dot{m}$ (kg/s)
1	Ammonia 98.9%, Water 6% (mass fraction)	369.03	3000	1059.9	0.05389
2	Ammonia 98.9%, Water 6% (mass fraction)	316.25	1084.7	1052.3	0.05389
3	Ammonia 70%, Water 30% (mass fraction)	324.31	1084.7	2957	0.2156
4	Ammonia 70%, Water 30% (mass fraction)	315.15	1084.7	2952.3	0.2156
5	Ammonia 70%, Water 30% (mass fraction)	315.71	3000	2952.9	0.2156
6	Ammonia 70%, Water 30% (mass fraction)	348.32	3000	2956.4	0.2156
7	Ammonia 70%, Water 30% (mass fraction)	369.03	3000	2970	0.2156
8	Ammonia 59%, Water 41% (mass fraction)	369.03	3000	1910.1	0.1617
9	Ammonia 59%, Water 41% (mass fraction)	325.71	3000	1905.2	0.1617
10	Ammonia 59%, Water 41% (mass fraction)	381.33	1084.7	1774.1	0.1617
11	Methane 90.4%, Ethane 5.4%, Propane 4.0%, Nitrogen 0.2% (mass fraction)	111.78	101.33	21,664	0.0825
12	Methane 90.4%, Ethane 5.4%, Propane 4.0%, Nitrogen 0.2% (mass fraction)	112.25	1215.9	21,664	0.0825
13	Methane 90.4%, Ethane 5.4%, Propane 4.0%, Nitrogen 0.2% (mass fraction)	293.15	1191.6	21,609	0.0825
14	Methane 90.4%, Ethane 5.4%, Propane 4.0%, Nitrogen 0.2% (mass fraction)	240.96	450	21,599	0.0825
15	Methane 90.4%, Ethane 5.4%, Propane 4.0%, Nitrogen 0.2% (mass fraction)	283.15	450	21,598	0.0825
16	Saline water (35,000 ppm)	288.15	101.3	0	2.921
17	Saline water (35,000 ppm)	288.15	650	1.566	2.921
18	Saline water (35,000 ppm)	288.15	625.7	1.497	2.921
19	Saline water (35,000 ppm)	288.15	603.29	1.4307	2.917
20	Saline water (35,000 ppm)	288.15	6000	16.772	2.917
21	Saline water (35,000 ppm)	288.15	625.7	0.002376	0.00463
22	Saline water (35,000 ppm)	288.15	180	0.000362	0.00463
23	Permeate water (350 ppm)	288.15	180	4.1902	1.602
24	Brine (77,350 ppm)	288.15	5100	8.2753	1.314
25	Brine (77,350 ppm)	288.15	101.3	2.0676	1.314
26	Product water (450 ppm)	288.15	180	4.1742	1.607
27	Product water (450 ppm)	288.15	101.3	4.0456	1.607
28	Saline water (35,000 ppm)	298.15	101.3	0	11.169
29	Saline water (35,000 ppm)	330.93	101.3	20.613	11.169
30	Saline water (35,000 ppm)	353.15	101.3	55.8563	11.169
31	Brine (36,861 ppm)	320.24	101.3	8.99	10.605
32	Humid air (relative humidity = 90%)	336.69	101.3	36.00	4.787
33	Humid air (relative humidity = 90%)	314.38	101.3	2.10	4.787
34	Pure water	325.53	101.3	1.18	0.563
	* TOTAL brine (41,327 ppm)	316.70	101.3	–	11.920
	* TOTAL freshwater (333 ppm)	297.86	101.3	–	2.170

Please cite this article as: Abbasi HR et al., Thermodynamic analysis of a tri-generation system using SOFC and HDH desalination unit, International Journal of Hydrogen Energy, https://doi.org/10.1016/j.ijhydene.2021.04.152

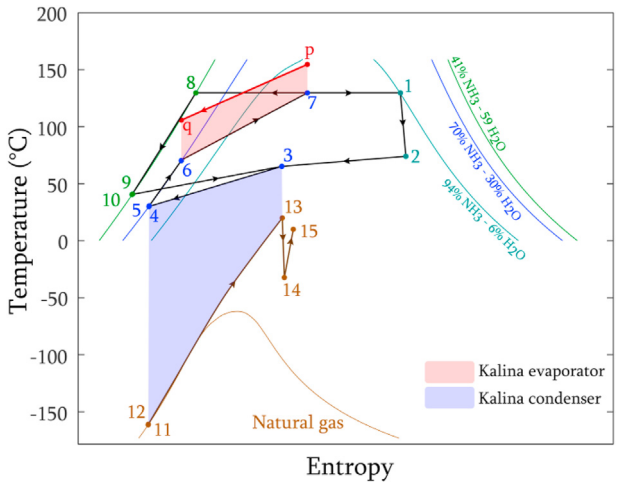

Fig. 4 – T-S diagram of the KC, LNG, and SOFC outlet flow.

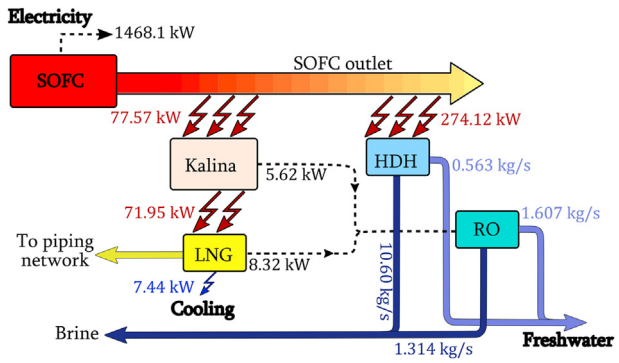

Fig. 5 – The schematic of the integrated system including the transferred heat and work.

$$\eta_{en} = \frac{\dot{W}_{grid} + \dot{Q}_{cooling} + (\dot{m}h)_{freshwater}}{\dot{Q}_{in}} \tag{30}$$

$$\eta_{ex} = \frac{\dot{W}_{grid} + \dot{E}x_{cooling} + \dot{E}x_{freshwater}}{\dot{E}x_{in}} \tag{31}$$

Results and discussions

To perform the simulation of the system and implement the governing equations, a mathematical code is developed in MATLAB software using REFPROP 9 library to predict the thermodynamic properties in each state. In the current study, a micro Pelton turbine is used to harvest the output energy of the high-pressure brine and the type of HDH unit is Open Water Close Air (OWCA). Detailed operating conditions and parameters of this integrated system are listed in Table 2.

Model validation

In this section, the KC has been already validated in previous articles by the authors [19,20], however, other cycles such as the SOFC need to be validated to obtain the simulation results.

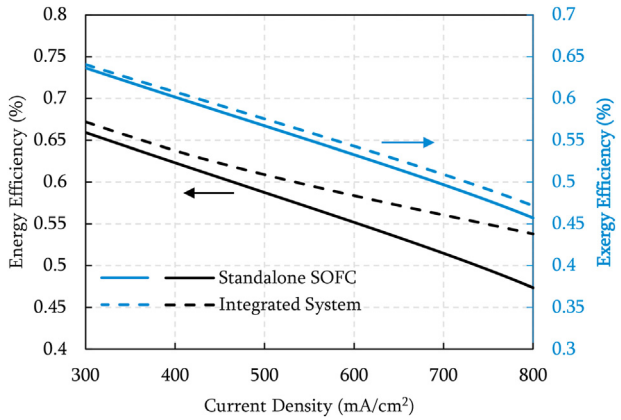

Fig. 6 – Energy and exergy efficiency of standalone SOFC and the integrated system and the effect of current density.

Fig. 2 validates the SOFC results compared to the data provided by Tao et al. [43]. The HDH unit is also validated in a previous investigation by the current authors [37] considering the developed research by Narayan et al. [44]. Fig. 3 validates the RO unit with the obtained data by Sharqawy et al. [45]. They assumed that the brine reject enters a high-pressure turbine that will provide the required power for the LPP in addition to utilizing two THVs to mitigate the pressure.

Thermodynamic analysis

Considering the input parameters of Table 2, a thermodynamic analysis of the system can be performed. In this regard, Table 3 presents the changes in the thermodynamic characteristics of the SOFC in all of its states. Table 4 also indicates the variation of temperature, pressure, exergy, and mass flow rate in all the states of the whole integrated system, regarding the changes in the compositions.

Figure 4 demonstrates the T-S diagram of the proposed system, which serves to illustrate the energy transfer in the system. Herein, the changes in the composition of the Kalina working fluid have been considered throughout the cycle by three colors. The results indicate that the ammonia-rich flow that goes through the expander has an ammonia mass fraction of 94%, while the ammonia-weak flow has a mass fraction of 41%. An important part of this figure is the illustrated saturation curve for the LNG stream. The existing large temperature difference between the ammonia-water mixture and LNG stream in the condenser of the KC results in a high rate of exergy distribution in this component.

Figure 5 illustrates a block diagram of the system including the amount of transferred heat and work between the subsystems. As the Kalina and HDH sub-systems are located along the SOFC outlet stream and in parallel to each other. The HDH unit needs a heat source with a lower temperature in comparison to the KC. Therefore, the HDH unit uses the waste heat at a lower temperature. The LNG cold stream provides the cooling of the domestic users by recovering the waste heat of the Kalina cycle while a share of the produced electricity will be given to the RO desalination unit to further produce freshwater. Fig. 5 shows that the SOFC generates 1468.1 kW electricity for

Please cite this article as: Abbasi HR et al., Thermodynamic analysis of a tri-generation system using SOFC and HDH desalination unit, International Journal of Hydrogen Energy, https://doi.org/10.1016/j.ijhydene.2021.04.152

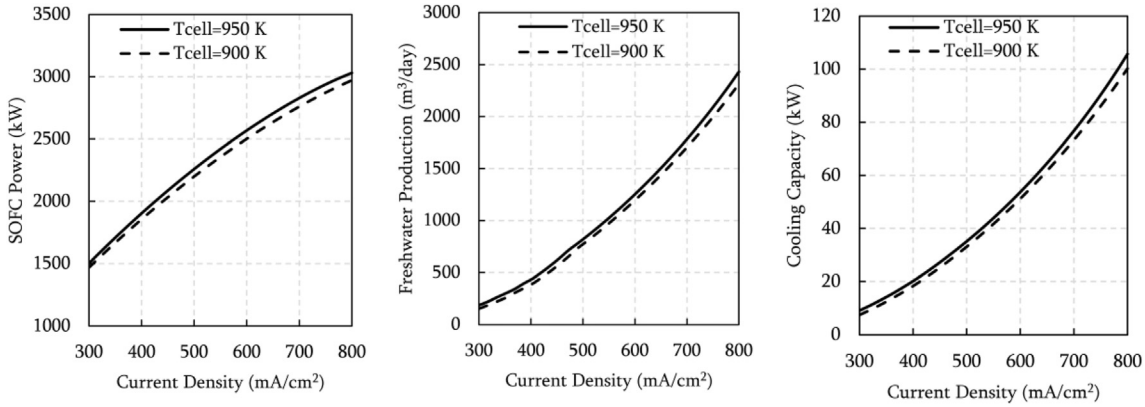

Fig. 7 – Effect of current density and operating temperature of fuel cell on three different productions of the integrated system.

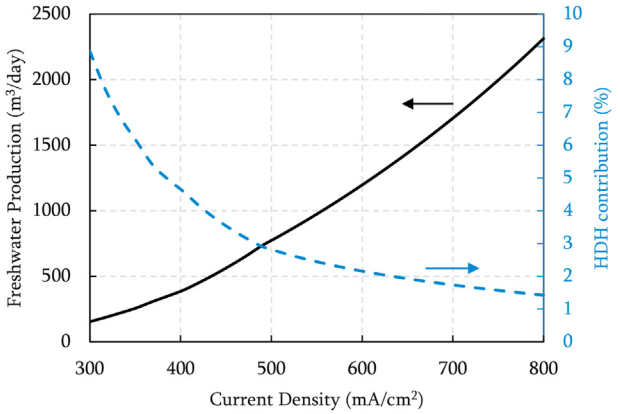

Fig. 8 – Freshwater production as a function of current density and contribution of HDH unit in freshwater production.

the grid while 351.69 of its waste heats can be recovered by Kalina cycle and HDH unit. As the exhaust temperature of the SOFC is not too high, it is not possible to use conventional Kalina cycles using high-temperatures as input. In this regard, small-scale Kalina units (~50 kW), which have been manufactured for low-temperature applications can be used in this suggested system. In addition to the utilization of the low-temperature Kalina cycles, other measures should be followed to implement this proposed system for a real application. In the Kalina cycle, although the separator separates the ammonia from the ammonia-water mixture, there would be still a mass fraction of water in the stream going to the Kalina's turbine. Therefore, incorporating the turbines designed for the working fluid of ammonia-water mixture is needed. A similar rule applies to the LNG stream and a turbine for the specific application of LNG is needed. Furthermore, HDH desalination units are usually being used for small-scale applications (less than 3 kg/h). For practical considerations, the single HDH unit analyzed in this study, could be a network of multiple HDH units working in parallel to each other. It is noteworthy to mention that RO units are the most commercialized desalination units among the available options in the market in different sizes and input electricity.

Figure 6 shows the energy and exergy efficiencies of a standalone SOFC without heat recovery and that of the integrated system for waste heat recovery considering changes in the current density. The figure shows there is a slight gain in the exergy efficiency regarding the waste heat recoveries, however, the improvement in the energy efficiency is more noticeable especially in high current densities.

Regarding the changes in the current density of the SOFC, results indicate that higher cell temperature reduces the overpotentials. Therefore, it is expected to have higher SOFC power for higher cell temperatures. It is noteworthy to mention that higher cell temperatures also increase the temperature of waste heat, which results in the operation of sub-cycles with increased capacity. Fig. 7 shows the enhancement in both freshwater production and cooling capacity by the increase in cell temperature.

Figures 8 and 9 show the contributions of each cycle to freshwater and power production, respectively. Fig. 8 clearly states that the contribution of the HDH unit in freshwater production is almost 9% at 300 mA/cm^2 while it reduces to lower than 2% by the enhancement in current density. Considering the high current densities, it is conceived that the

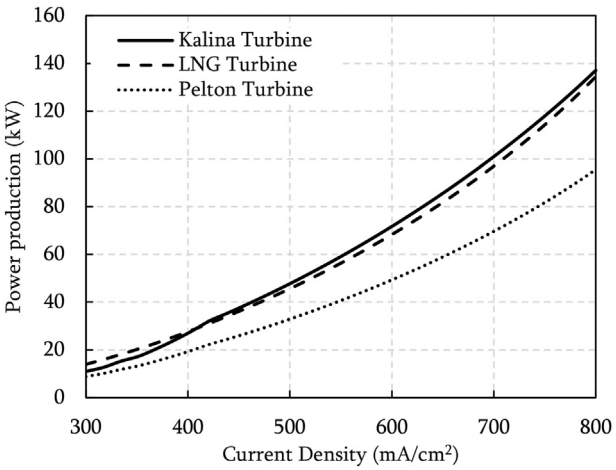

Fig. 9 – Comparison of power production of three different turbines in an integrated system with cell temperature of 900K.

Please cite this article as: Abbasi HR et al., Thermodynamic analysis of a tri-generation system using SOFC and HDH desalination unit, International Journal of Hydrogen Energy, https://doi.org/10.1016/j.ijhydene.2021.04.152

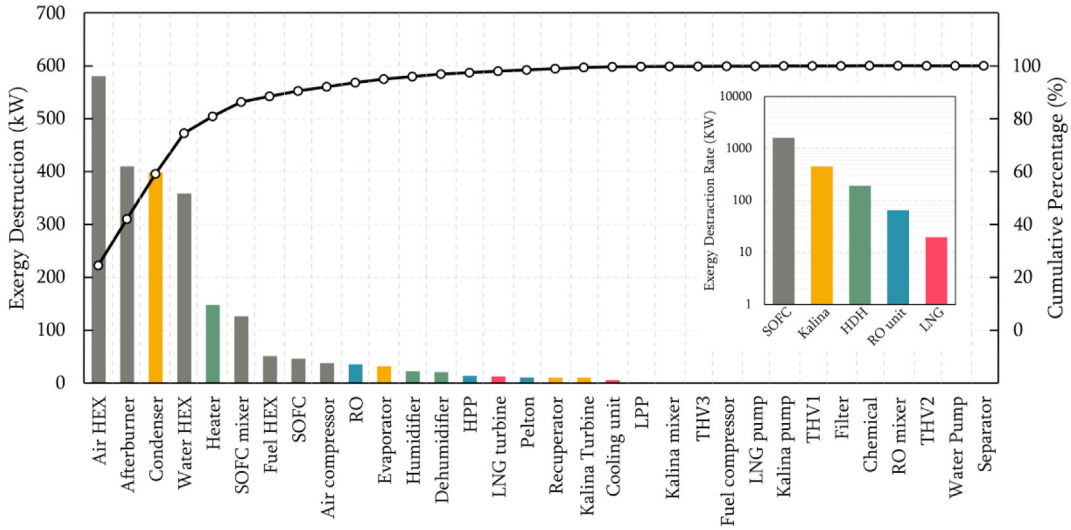

Fig. 10 – Rate of exergy destruction for all components in the system.

role of RO in freshwater production is more substantial. Fig. 9 also shows the output power of the three implemented turbines in the system, where the Kalina turbine has by far the highest output at high current densities. For low current densities, the LNG stream turbine has the highest output power, while the Pelton turbine of the RO unit has the lowest output for all current densities of the SOFC.

In every multi-generation system, exergy analysis is needed to figure out the efficiency of the utilized components. Fig. 10 demonstrates the exergy destruction rate of each component and its contribution to the total exergy destruction of the integrated system. The inserted histogram shows the exergy destruction rate of each sub-cycle have the highest exergy destruction rates in the system, while among the components, five are responsible for more than 80% of total exergy destruction: air heat exchanger, afterburner, Kalina condenser, water heat exchanger, and water heater in HDH cycle.

Conclusions

In this study, the thermodynamic analysis of a novel multi-generation system to simultaneously produce power, cooling, and freshwater was performed. This state-of-the-art system enables producing freshwater by both heat and electricity as a result of using HDH and RO desalination units, respectively. The integration of the Kalina cycle also improves the waste heat recovery of the SOFC to further generate electricity. This system has not been evaluated yet, hence energy and exergy analyzes of this system were performed.

The T-S diagram of the current system indicates that the ammonia-rich flow that goes through the expander has an ammonia mass fraction of 94%, while the ammonia-weak flow has a mass fraction of 40%. It also illustrates that the high exergy destruction rate of the KC condenser is a result of the high temperature difference between the ammonia-water mixture and LNG streams. Exergy analysis of the system stated the positive effects of integrating a KC and HDH desalination unit to recover the waste heat of a SOFC, which resulted in higher exergy efficiencies. Considering the changes in current density and the SOFC temperature, it was shown that higher cell temperatures mitigate the SOFC's output power while both freshwater production and cooling capacity are improved. In this integration and the implementation of both HDH and RO units to produce freshwater, it is conceived that the share of the HDH unit is not dominant in which it has a contribution of 9% at low current densities reduced to 2% at high current densities. To understand the working efficiency of the turbines in the system, it was also determined that the Kalina turbine has by far the highest output at high current densities, while for low current densities, the LNG stream turbine has the highest output power. The analysis of the exergy destruction rate determined that the SOFC unit has by far the highest exergy destruction rate, while the LNG stream has the lowest. Finally, it was shown that five components (air heat exchanger, afterburner, Kalina condenser, water heat exchanger, and the water heater in the HDH cycle) combine to a >80% share of total exergy destruction.

Although thermodynamic analysis gives an overall overview about the appropriateness and the performance of a system, the implementation of any multi-generation system in reality demands economic analysis as well. In this regard, performing any type of economic evaluation such as exergo-economic, or thermo-economic is appreciated to further analyze this system. Additionally, a comprehensive comparison can be made with the other suggested tri-generation systems, which produce power, freshwater, and cooling, considering energy, exergy, and economic aspects.

Declaration of competing interest

The authors declare the following financial interests/personal relationships, which may be considered as potential competing interests: This project has received funding from the European Union's Horizon 2020 research and innovation program under the Marie Sklodowska-Curie grant agreement No. 754354.

Please cite this article as: Abbasi HR et al., Thermodynamic analysis of a tri-generation system using SOFC and HDH desalination unit, International Journal of Hydrogen Energy, https://doi.org/10.1016/j.ijhydene.2021.04.152

Acknowledgment

This project received funding from the European Union's Horizon 2020 research and innovation program under the Marie Sklodowska-Curie grant agreement No. 754354.

Nomenclature

ζ_{act}	Activation overpotential (V)
ζ_{conc}	Concentration overpotential (V)
ζ_{ohm}	Ohmic overpotential (V)
A_{act}	Activation area (m^2)
i	Current density (A/m^2)
N_{cell}	Number of cells
R_r	Recovery ratio
V_N	Reversible voltage (V)
V_{cell}	Cell's voltage (V)
V_{loss}	Voltage losses (V)
$\dot{W}_{SOFC}$	Output power of SOFC (W)
y_s	Mass fraction of salt

Abbreviation

CPVT	Concentrated Photovoltaic Thermal
GOR	Gained output ratio
GT	Gas Turbine
HDH	Humidification-dehumidification
HPP	High-pressure pump
KC	Kalina cycle
LNG	Liquefied Natural Gas
LPP	Low-pressure pump
MED	Multi-Effect Desalination
OWCA	Open Water Close Air
PEMFC	Proton Exchange Membrane Fuel Cell
RO	Reverse Osmosis
SOFC	Solid Oxide Fuel Cell
TEG	Thermoelectric generator
THV	Throttle valve

REFERENCES

[1] Rokni M. Analysis of a polygeneration plant based on solar energy, dual mode solid oxide cells and desalination. Int J Hydrogen Energy Jul. 2019;44(35):19224–43. https://doi.org/10.1016/j.ijhydene.2018.03.147.

[2] Liu G, Sheng Y, Ager JW, Kraft M, Xu R. Research advances towards large-scale solar hydrogen production from water. EnergyChem Sep. 2019;1(2):100014. https://doi.org/10.1016/j.enchem.2019.100014.

[3] Zhao X, et al. Fabrication, characteristics and applications of carbon materials with different morphologies and porous structures produced from wood liquefaction: a review. Chem Eng J May 2019;364:226–43. https://doi.org/10.1016/j.cej.2019.01.159.

[4] Li H. Porous metal-organic frameworks for gas storage and separation. Status Chall 2019:39.

[5] Wang H-F. MOF-derived electrocatalysts for oxygen reduction, oxygen evolution and hydrogen evolution reactions. Chem Soc Rev 2020:36.

[6] Roushenas R, Razmi AR, Soltani M, Torabi M, Dusseault MB, Nathwani J. Thermo-environmental analysis of a novel cogeneration system based on solid oxide fuel cell (SOFC) and compressed air energy storage (CAES) coupled with turbocharger. Appl Therm Eng Nov. 2020;181:115978. https://doi.org/10.1016/j.applthermaleng.2020.115978.

[7] Weber A, Szasz J, Dierickx S, Endler-Schuck C, Ivers-Tiffee E. Accelerated lifetime tests for SOFCs. ECS Trans Jul. 2015;68(1):1953–60. https://doi.org/10.1149/06801.1953ecst.

[8] Inac S, Unverdi SO, Midilli A. Global warming, environmental and sustainability aspects of a geothermal energy based biodigester integrated SOFC system. Int J Hydrogen Energy Dec. 2020;45(60):35039–52. https://doi.org/10.1016/j.ijhydene.2020.06.224.

[9] El-Emam RS, Dincer I, Naterer GF. Energy and exergy analyses of an integrated SOFC and coal gasification system. Int J Hydrogen Energy Jan. 2012;37(2):1689–97. https://doi.org/10.1016/j.ijhydene.2011.09.139.

[10] Pourrahmani H, Siavashi M, Moghimi M. Design optimization and thermal management of the PEMFC using artificial neural networks. Energy Sep. 2019;182:443–59. https://doi.org/10.1016/j.energy.2019.06.019.

[11] Pourrahmani H, Moghimi M, Siavashi M, Shirbani M. Sensitivity analysis and performance evaluation of the PEMFC using wave-like porous ribs. Appl Therm Eng Mar. 2019;150:433–44. https://doi.org/10.1016/j.applthermaleng.2019.01.010.

[12] Pourrahmani H, Moghimi M, Siavashi M. Thermal management in PEMFCs: the respective effects of porous media in the gas flow channel. Int J Hydrogen Energy Jan. 2019;44(5):3121–37. https://doi.org/10.1016/j.ijhydene.2018.11.222.

[13] Bicer Y, Dincer I. Energy and exergy analyses of an integrated underground coal gasification with SOFC fuel cell system for multigeneration including hydrogen production. Int J Hydrogen Energy Oct. 2015;40(39):13323–37. https://doi.org/10.1016/j.ijhydene.2015.08.023.

[14] Adebayo V, Abid M, Adedeji M, Hussain Ratlamwala TA. Energy, exergy and exergo-environmental impact assessment of a solid oxide fuel cell coupled with absorption chiller & cascaded closed loop ORC for multi-generation. Int J Hydrogen Energy Mar. 2021. https://doi.org/10.1016/j.ijhydene.2021.02.222. S0360319921008156.

[15] Yang X, Zhao H, Hou Q. Proposal and thermodynamic performance study of a novel LNG-fueled SOFC-HAT-CCHP system with near-zero CO2 emissions. Int J Hydrogen Energy Jul. 2020;45(38):19691–706. https://doi.org/10.1016/j.ijhydene.2020.05.012.

[16] Haseli Y, Dincer I, Naterer GF. Thermodynamic analysis of a combined gas turbine power system with a solid oxide fuel cell through exergy. Thermochim Acta Dec. 2008;480(no. 1–2):1–9. https://doi.org/10.1016/j.tca.2008.09.007.

[17] Saebea D, Arpornwichanop A, Patcharavorachot Y. Thermodynamic analysis of a proton conducting SOFC integrated system fuelled by different renewable fuels. Int J Hydrogen Energy Mar. 2021;46(20):11445–57. https://doi.org/10.1016/j.ijhydene.2020.07.264.

[18] Palsson J, Selimovic A, Sjunnesson L. Combined solid oxide fuel cell and gas turbine systems for efficient power and heat generation. J Power Source 2000:7.

[19] Emadi MA, Pourrahmani H, Moghimi M. Performance evaluation of an integrated hydrogen production system with LNG cold energy utilization. Int J Hydrogen Energy Dec. 2018;43(49):22075–87. https://doi.org/10.1016/j.ijhydene.2018.10.048.

[20] Abbasi HR, Pourrahmani H, Yavarinasab A, Emadi MA, Hoorfar M. Exergoeconomic optimization of a solar driven system with reverse osmosis desalination unit and phase change material thermal energy storages. Energy Convers

Please cite this article as: Abbasi HR et al., Thermodynamic analysis of a tri-generation system using SOFC and HDH desalination unit, International Journal of Hydrogen Energy, https://doi.org/10.1016/j.ijhydene.2021.04.152

Manag Nov. 2019;199:112042. https://doi.org/10.1016/j.enconman.2019.112042.
[21] Pourrahmani H, Moghimi M. Exergoeconomic analysis and multi-objective optimization of a novel continuous solar-driven hydrogen production system assisted by phase change material thermal storage system. Energy Dec. 2019;189:116170. https://doi.org/10.1016/j.energy.2019.116170.
[22] Ma S, Wang J, Yan Z, Dai Y, Lu B. Thermodynamic analysis of a new combined cooling, heat and power system driven by solid oxide fuel cell based on ammonia–water mixture. J Power Sources Oct. 2011;196(20):8463–71. https://doi.org/10.1016/j.jpowsour.2011.06.008.
[23] Soltani M. A comparative study between ORC and Kalina based waste heat recovery cycles applied to a green compressed air energy storage (CAES) system. Energy Convers Manag 2020:19.
[24] Abam FI, et al. Thermodynamic and economic analysis of a Kalina system with integrated lithium-bromide-absorption cycle for power and cooling production. Energy Rep Nov. 2020;6:1992–2005. https://doi.org/10.1016/j.egyr.2020.07.021.
[25] Dhahad HA, Hussen HM, Nguyen PT, Ghaebi H, Ashraf MA. Thermodynamic and thermoeconomic analysis of innovative integration of Kalina and absorption refrigeration cycles for simultaneously cooling and power generation. Energy Convers Manag Jan. 2020;203:112241. https://doi.org/10.1016/j.enconman.2019.112241.
[26] Ghaebi H, Parikhani T, Rostamzadeh H, Farhang B. Thermodynamic and thermoeconomic analysis and optimization of a novel combined cooling and power (CCP) cycle by integrating of ejector refrigeration and Kalina cycles. Energy Nov. 2017;139:262–76. https://doi.org/10.1016/j.energy.2017.07.154.
[27] Lin W, Huang M, Gu A. A seawater freeze desalination prototype system utilizing LNG cold energy. Int J Hydrogen Energy Jul. 2017;42(29):18691–8. https://doi.org/10.1016/j.ijhydene.2017.04.176.
[28] Atsonios K. Technical assessment of LNG based polygeneration systems for non-interconnected island cases using SOFC. Int J Hydrogen Energy 2021:17.
[29] Ghaebi H, Namin AS, Rostamzadeh H. Exergoeconomic optimization of a novel cascade Kalina/Kalina cycle using geothermal heat source and LNG cold energy recovery. J Clean Prod Jul. 2018;189:279–96. https://doi.org/10.1016/j.jclepro.2018.04.049.
[30] Abbasi HR, Pourrahmani H. Multi-objective optimization and exergoeconomic analysis of a continuous solar-driven system with PCM for power, cooling and freshwater production. Energy Convers Manag May 2020;211:112761. https://doi.org/10.1016/j.enconman.2020.112761.
[31] Chitgar N, Emadi MA, Chitsaz A, Rosen MA. Investigation of a novel multigeneration system driven by a SOFC for electricity and fresh water production. Energy Convers Manag Sep. 2019;196:296–310. https://doi.org/10.1016/j.enconman.2019.06.006.
[32] Mokhtari H, Sepahvand M, fasihfar A. Thermoeconomic and exergy analysis in using hybrid systems (GT + MED + RO) for desalination of brackish water in Persian Gulf. Desalination Dec. 2016;399:1–15. https://doi.org/10.1016/j.desal.2016.07.044.
[33] Sadri S, Ameri M, Haghighi Khoshkhoo R. Multi-objective optimization of MED-TVC-RO hybrid desalination system based on the irreversibility concept. Desalination Jan. 2017;402:97–108. https://doi.org/10.1016/j.desal.2016.09.029.
[34] Eshoul NM, Agnew B, Anderson A, Atab MS. Exergetic and economic analysis of two-pass RO desalination proposed plant for domestic water and irrigation. Energy Mar. 2017;122:319–28. https://doi.org/10.1016/j.energy.2017.01.095.
[35] Altmann T, Robert J, Bouma A, Swaminathan J, Lienhard JH. Primary energy and exergy of desalination technologies in a power-water cogeneration scheme. Appl Energy Oct. 2019;252:113319. https://doi.org/10.1016/j.apenergy.2019.113319.
[36] Alirahmi SM, Assareh E. Energy, exergy, and exergoeconomics (3E) analysis and multi-objective optimization of a multi-generation energy system for day and night time power generation - case study: Dezful city. Int J Hydrogen Energy Nov. 2020;45(56):31555–73. https://doi.org/10.1016/j.ijhydene.2020.08.160.
[37] Abbasi HR, Pourrahmani H. Multi-criteria optimization of a renewable hydrogen and freshwater production system using HDH desalination unit and thermoelectric generator. Energy Convers Manag Jun. 2020;214:112903. https://doi.org/10.1016/j.enconman.2020.112903.
[38] Moumouh J, Tahiri M, Salouhi M. Solar thermal energy combined with humidification–dehumidification process for desalination brackish water: technical review. Int J Hydrogen Energy Sep. 2014;39(27):15232–7. https://doi.org/10.1016/j.ijhydene.2014.04.216.
[39] Ghofrani I, Moosavi A. Energy, exergy, exergoeconomics, and exergoenvironmental assessment of three brine recycle humidification-dehumidification desalination systems applicable for industrial wastewater treatment. Energy Convers Manag Feb. 2020;205:112349. https://doi.org/10.1016/j.enconman.2019.112349.
[40] Elsafi AM. Integration of humidification-dehumidification desalination and concentrated photovoltaic-thermal collectors: energy and exergy-costing analysis. Desalination Dec. 2017;424:17–26. https://doi.org/10.1016/j.desal.2017.09.022.
[41] Deniz E, Çınar S. Energy, exergy, economic and environmental (4E) analysis of a solar desalination system with humidification-dehumidification. Energy Convers Manag Oct. 2016;126:12–9. https://doi.org/10.1016/j.enconman.2016.07.064.
[42] Ghaebi H, Ahmadi S. Energy and exergy evaluation of an innovative hybrid system coupled with HRSG and HDH desalination units. J Clean Prod Apr. 2020;252:119821. https://doi.org/10.1016/j.jclepro.2019.119821.
[43] Tao G, Armstrong T, Virkar A. Intermediate temperature solid oxide fuel cell (IT-SOFC) research and development activities at MSRI. In: Ninet Annu ACERCICES Conf; 2005.
[44] Narayan GP, Sharqawy MH, Lienhard V JH, Zubair SM. Thermodynamic analysis of humidification dehumidification desalination cycles. Desalinat Water Treat Apr. 2010;16(no. 1–3):339–53. https://doi.org/10.5004/dwt.2010.1078.
[45] Sharqawy MH, Zubair SM, Lienhard JH. Second law analysis of reverse osmosis desalination plants: an alternative design using pressure retarded osmosis. Energy Nov. 2011;36(11):6617–26. https://doi.org/10.1016/j.energy.2011.08.056.

Please cite this article as: Abbasi HR et al., Thermodynamic analysis of a tri-generation system using SOFC and HDH desalination unit, International Journal of Hydrogen Energy, https://doi.org/10.1016/j.ijhydene.2021.04.152